OVERVIEW OF MEERKAT L-BAND AND U-BAND NONLINEARITY

Document number M0000-0000-092
Revision 1
Classification ..... Commercial in Confidence
Prepared By ..... M Gouws

Approval Date ..... 07 December 2020

Organisation	:	NRF (National Research Foundation)
Facility	:	SARAO (South African Radio Astronomy Observatory)
Project	:	MeerKAT
Document Type	:	Report
Function/Discipline	:	Systems Engineering

DOCUMENT APPROVALS

	Name	Designation	Affiliation	Date	Signature
Released By	Marcel Gouws mgouws@ska.ac.za	Senior Systems Analyst	SARAO	Feb 5, 2021	Marcel Gouws Marcel Gouws (Feb 5, 2021 21:53 GMT+2)
Accepted By					
Approved By					

DOCUMENT HISTORY

Revision	Date Of Issue	Prepared By	Comments (e.g. ECN Number or changes to document)

DOCUMENT DISTRIBUTION

DOCUMENT SOFTWARE

Package		Version	Filename
Word Processor	Ms Word	Word 2007	Overview of MeerKAT L-band and U-band Nonlinearity Rev 1.docx

COMPANY DETAILS

Name	SARAO, Johannesburg Office (Rosebank, Gauteng)	SARAO, Cape Town (Observatory, Cape Town)	SARAO, HartRAO (Hartebeeshoek, Gauteng)	SARAO, Karoo Astronomy Reserve (Carnarvon, Northern Cape)
Physical / Postal Address	1st Floor, 17 Baker Street Rosebank, Gauteng 2196, South Africa	2 Fir Street, (North Entrance Black River Park, Observatory, Cape Town, 7925	P.O.Box 443, Krugersdorp, 1740, South Africa	Posbus 69, Carnarvon, 8925, South Africa
Tel.	27 11 268 3400	+27 21 506 7300	+27 12 301 3100	+27 21 506 7300
Fax.	27 11 442 2454	+27 21 506 7375	+27 12 301 3300	+27 86 538 6836
Website	www.ska.ac.za	www.ska.ac.za	www.hartrao.ac.za	www.ska.ac.za

TABLE OF CONTENTS

LIST OF FIGURES

ABBREVIATIONS

ADC	Analog to Digital Converter
CW	Continuous Wave
FDD	Frequency Division Duplex
FFT	Fast Fourier Transform
GNSS	Global Navigation Satellite System
GPS	Global Positioning System
GSM	Global System for Mobile Communication
INL	Integral Nonlinearity
LTE	Long Term Evolution
RFCU	Radio Frequency Conditioning Unit
RFI	Radio Frequency Interference
SDP	Science Data Processor
SEFD	System Equivalent Flux Density
TLE	Two-line Element
UMTS	Universal Mobile Telecommunications Service

1 INTRODUCTION

MeerKAT L-band and U-band receivers experience significant gain instability in response to variable input power, with most receivers [1] not meeting the linearity performance specification (R.RC.P31 in [2]). Previous telescope-level investigations in L-band [3] and U-band [4] found that the source of the nonlinearity is most likely located within the Digitiser subsystem, and laboratory experiments [5] pointed to the ADC as the cause.

This document summarises main results from L-band and U-band test observations, as illustration of the possible impact of nonlinear behaviour for telescope users. Possible methods to compensate for the nonlinear effects are also noted.

Section 2 presents examples of observed nonlinear behaviour, with remaining open questions noted in Section 3. Possible consequences of these effects for users are discussed in Section 4. Section 5 notes possible mitigating measures currently under consideration.

2 OBSERVED NONLINEAR EFFECTS

Observed nonlinear effects inherently entail variation in receiver gain in response to significant changes in ADC input power. This section illustrates key scenarios where variation in input power comes into play, as basis for discussing consequences for telescope users.

2.1 SATELLITE RFI

RFI from satellite-borne transmitters within the antenna main beam or close-in sidelobes may cause large changes in receiver input power, leading to significant gain instability. This is only a concern in L-band, primarily for GNSS satellites, since offending frequency bands are removed by U-band bandpass filtering prior to the ADC.

Figure 1 demonstrates typical variation in interferometric gains[1] for selected antennas as a GPS satellite passes through the antenna main beams. Also shown is variation of mean power in an RFI-free band, which changes in step with receiver gain. Gains and RFI-free power are normalised to their values at the start of the measurement to illustrate relative variation. Figure 1 shows that increases in gain of order 10% are common. Furthermore, considering m048v and m053h in the figure, it's clear that the response can vary dramatically from one receiver to the next, which was attributed in [5] to a differing Integrated Nonlinearity (INL) response between ADCs.

[1] Calculated every 32 seconds by MeerKAT SDP calibration pipeline while tracking calibrator J1939-6342. Receiver gain relates to interferometric broadband "voltage gain" g as $|g|^2$.

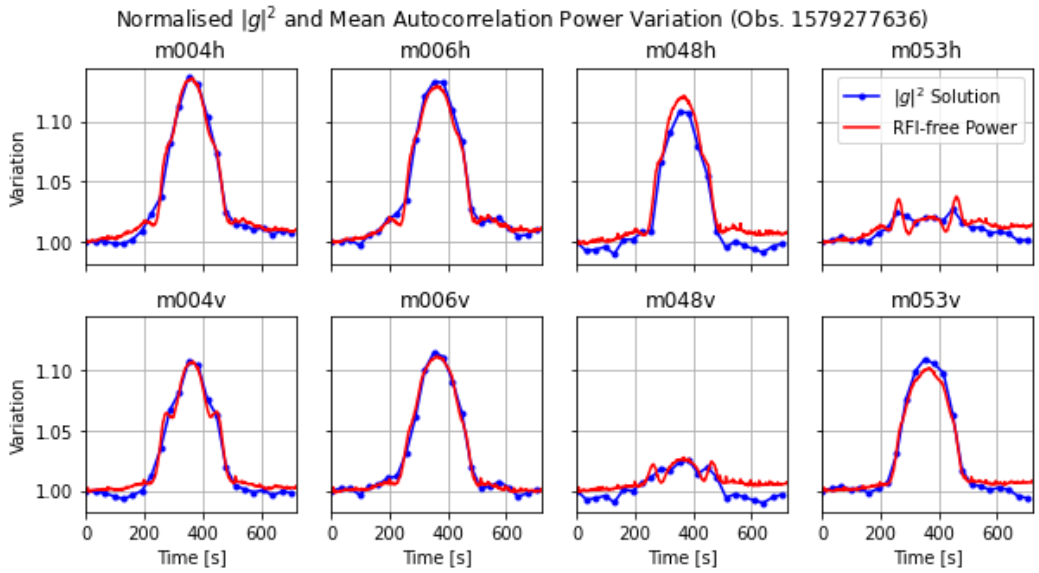

Figure 1 – Interferometric gain variation in response to GNSS RFI.

Satellites crossing the main beam provide a large variation in input power over short time scales during which gain drift due to other effects might be assumed negligible. Hence such events provide a useful measurement of how gain varies as a function of ADC input power, as shown in Figure 2 for selected antennas. Note that most antennas show an approximate linear gain increase of ~0.66 % per dB increase in ADC input power. This is a useful rough guideline to guide expectations for nonlinear effects in L-band.

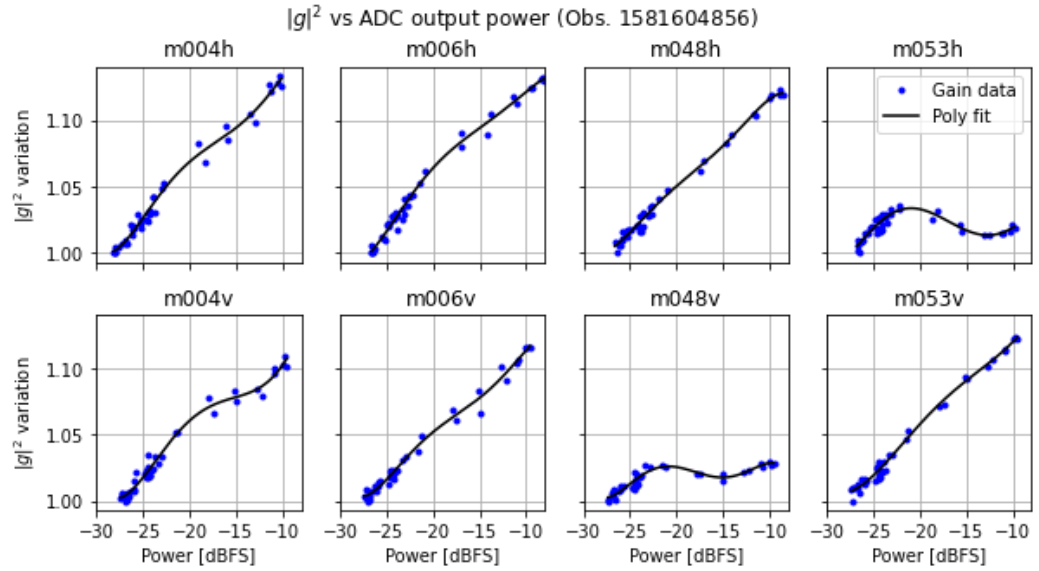

Figure 2 – Interferometric gain vs. ADC input power as a result of GNSS RFI.

2.2 NOISE DIODE

The noise diode is a significant source of power variation for both L-band and U-band receivers, known to increase power levels by approximately 3 dB when firing[2]. The consequence is that receiver gain differs when the noise diode is fired. Figure 3 illustrates the ratio between $|g_{ON}|^2$, interferometric gain when the noise diode is on, and $|g_{OFF}|^2$, interferometric gain when the noise diode is off for L-band. Although significant variation is seen across inputs, the median response is an increase in gain of ~2%. U-band displays very similar results.

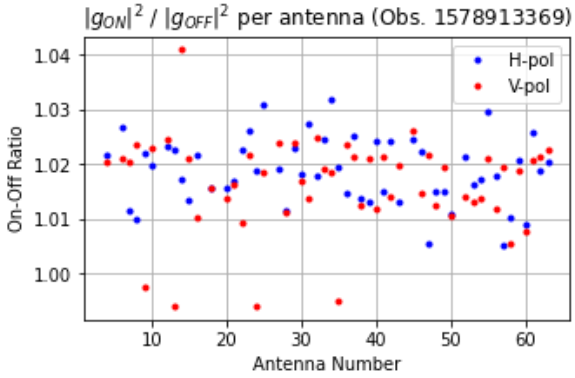

Figure 3 – Ratio of gains with noise diode on vs. off, L-band.

Noise diode power P_{ND} is often measured as a convenient means to track changes in receiver gain, relying on the assumption $P_{ND} \sim G(T_{ON} - T_{OFF})$, where G represents receiver gain and T_{ON} and T_{OFF} respectively system temperature when the noise diode is on and off. If firing the noise diode changes receiver gain, we however have $P_{ND} \sim G_{OFF}\left(\frac{G_{ON}}{G_{OFF}}T_{ON} - T_{OFF}\right)$, with distinctly varying gains G_{ON} and G_{OFF}. Variation in measured P_{ND} hence differs from that G_{OFF}, the gain when the noise diode is not firing.

Figure 4 shows an example of inaccuracy in P_{ND} variation for noise diode power measurements while a GNSS satellite drifts through the antenna main beam. Here $P_{ND} = P_{ON} - P_{OFF}$, with P_{ON} and P_{OFF} respectively the mean RFI-free autocorrelation power when the noise diode is on and off. P_{OFF} variation is here assumed approximately equal to variation in receiver gain G_{OFF} brought about by the GNSS RFI[3]. Significant differences between variation in P_{ND} and P_{OFF} are apparent, unlike the close correspondence between interferometric gains and RFI-free power variation demonstrated in Figure 1.

[2] At selected nominal input power settings.

[3] Ignoring the comparatively small variation due to the sky drifting through the beam during this measurement.

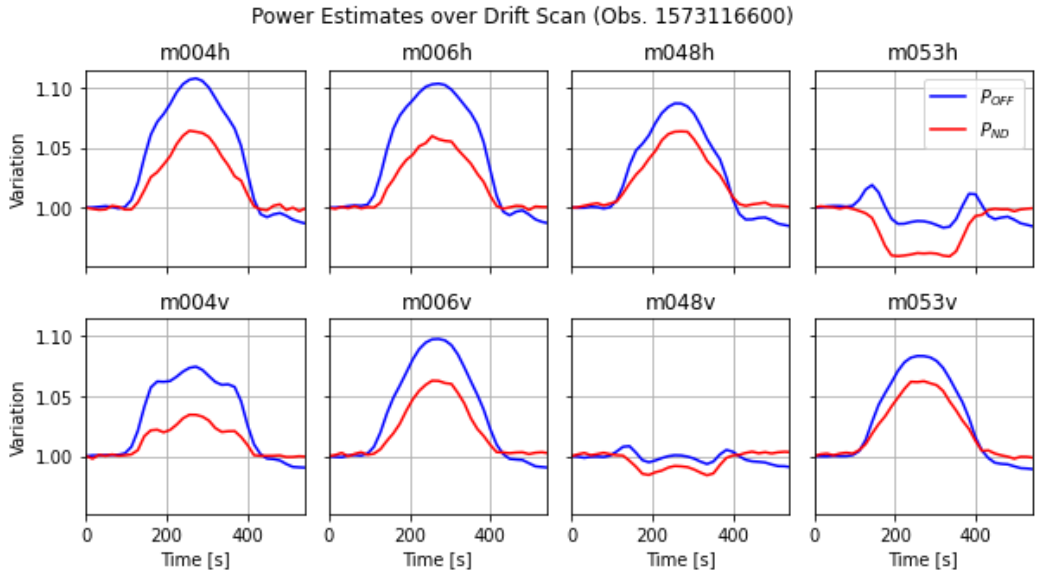

Figure 4 – Variation in noise diode power measurements across a GNSS drift scan.

2.3 T_{SYS} VARIATION

Large changes in T_{SYS} will lead to variations in receiver gain in both L-band and U-band. Increases in ADC input power of order 3 dB or more above nominal are often measured when the galactic plane or other bright extended sources are in beam. Subtler elevation-dependent variation might be present due to spillover or atmospheric effects, though this still has to be characterised in detail.

Figure 5 illustrates variation in noise diode power P_{ND} across a drift scan of Tau A for selected antennas in U-band[4]. This suggests variations in gain of order 3% or more are present, noting that results from Section 2.2 suggest this would likely be an underestimation of gain variation.

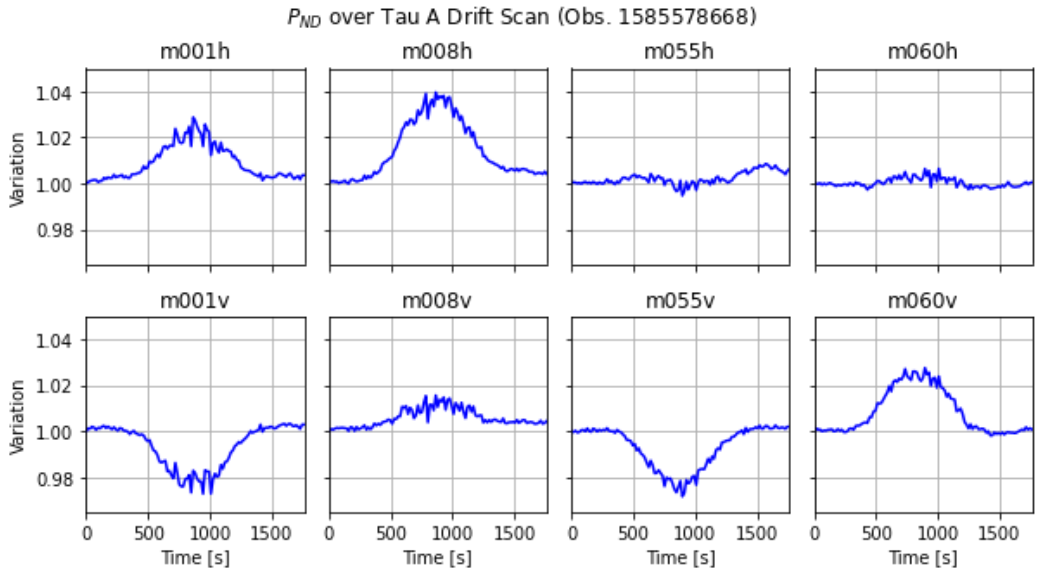

Figure 5 – P_{ND} variations across U-band Tau A drift scan.

[4] The 'noisy' P_{ND} values during this measurement was suspected to be an issue with noise diode synchronisation.

2.4 PERSISTENT RFI

Cell tower transmissions are the dominant source of persistent RFI causing input power variation on short time scales, with main culprits for MeerKAT being UMTS and GSM downlinks in the 935-944 MHz band. Power received varies with pointing direction and cell tower activity. Variation with pointing direction still needs to be characterised, though when integrated to correlator dump intervals, typical input power variation over time caused by cellular RFI is of order 0.1 dB[5]. On such time scales, RMS gain variation caused by cell tower RFI is hence expected to be small and not of particular concern.

However, power received from cell tower RFI may vary periodically on millisecond time-scales according to the data frame structure of protocols, most notably:

- GSM: a 120/26 ms frame, divided into 8 time slots.
- UMTS: a 10 ms frame, divided into 15 time slots.
- LTE (FDD): a 10 ms frame, divided into 20 time slots.

Folding FFT-channelised digitiser data on a period equal to the GSM time slot (T_{fold} = 0,576 ms) confirms the presence of significant periodic variation in total receiver power, leading to variation in gain. Figure 6 illustrates the deviation of power from the median in a channel (top panel), deviation in RFI power (middle panel), as well as in total power and mean RFI-free power (bottom panel). Total received power drops by 0.75 dB due to ~14 dB variation in the 942-944 MHz GSM band. The total power drop coincides with broadband drop in RFI-free power of 0.5%. This is consistent with the expected gain variation from ADC nonlinearity of 0.66% per dB input power variation noted in Section 2.1.

[5] Median 5-σ variation across antennas after compensation for linear drift on 0.5 second correlator dumps across 5 minute windows during a low-elevation observation.

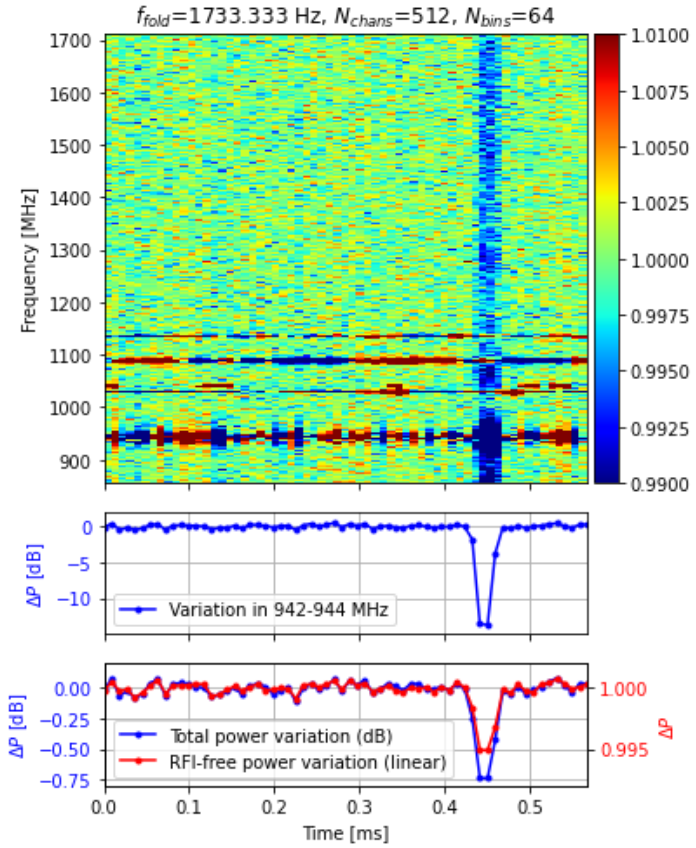

Figure 6 – Folded L-band digitiser capture from m004v (T_{INT} = 8 s), showing deviation from median power in each channel (top panel) and deviation from median power in selected bands over time (middle and bottom panels).

Cellular RFI signals arrive at different antennas with different propagation delays. Considering that propagation across MeerKAT's 1 km core takes only 3.3 us, millisecond-scale variations in RFI power will still be approximately aligned in time for many antennas. Hence gain modulation is expected to be present in MeerKAT beamformer data. Folding captures of beamformer data at the appropriate periods, shown in Figure 7, confirms presence in beamformer data of (a) strong gain variation within GSM time slots, (b) detectable variation within UMTS time slots, and (c) strong variation within GSM data frames.

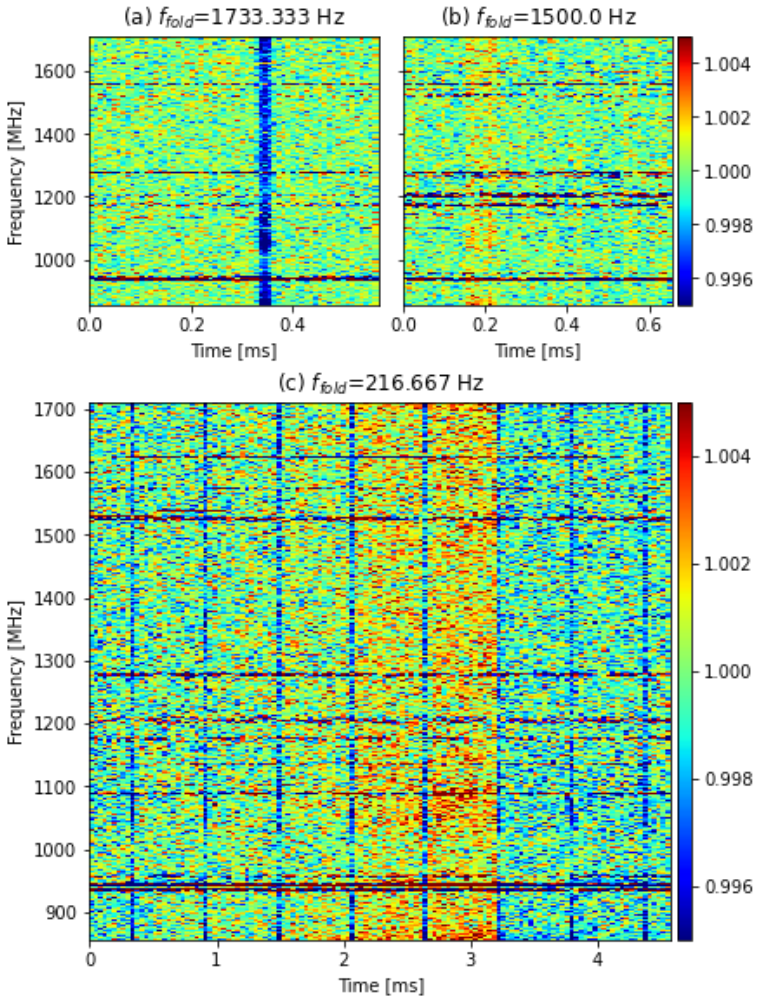

Figure 7 – Deviation from channel median power in 1K beamformer data folded (T_{INT} = 60 s) at a period of (a) the GSM time code, (b) UMTS time code, and (c) GSM data frame.

3 REMAINING UNCERTAINTIES

Greater than anticipated receiver nonlinearity may imply that levels of intermodulation products between RFI are higher than expected. This still needs to be investigated in detail.

Variation of input power with pointing direction needs to be characterised, with regards to both (i) received cell tower RFI and (ii) variation due to spillover or atmospheric effects.

Significant variation in bandpass gains are consistently observed in L-band when input power increases significantly. This is most clearly demonstrated by comparing interferometric bandpass solutions when a GNSS satellite is in-beam vs out-of-beam, as shown in Figure 8. A similar response is seen on all L-band receivers, showing possible resonant peaks are seen at intervals of ~140 MHz. These are not merely calibration artefacts, as they are also seen when comparing noise diode spectra when a GNSS satellite is in-beam vs out-of-beam. It's not immediately obvious how this might be attributed to ADC nonlinearity, and the cause is unclear at present. Laboratory experiments with a U-band digitiser [5] did not show any bandpass spectrum variation, even with

severe CW interference. Further investigation is required, in particular laboratory measurements with an L-band digitiser. Measurement of noise diode spectra at high and low T_{SYS} may be attempted to confirm that the effect is absent in U-band.

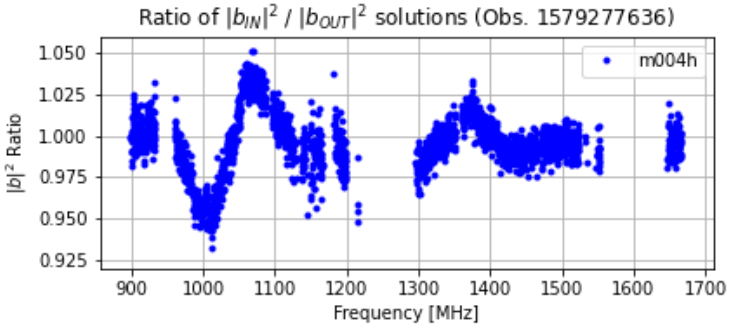

Figure 8 – Ratio of L-band bandpass solutions with a GNSS satellite in-beam vs. out-of-beam.

During measurements to check the influence of the noise diode on interferometric gains, it was found that some receivers also display variation in gain phase, not merely magnitude, when the noise diode was on vs off. This is observed both in L-band and U-band, as shown in Figure 9 for U-band. Trends in gain phase are not obviously present within L-band GNSS measurements. At present it cannot be conclusively stated that the observed nonlinearity also includes phase variation, though this will be investigated further.

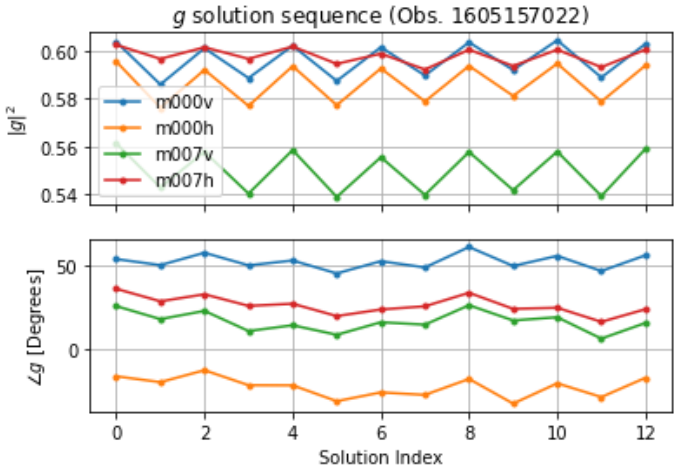

Figure 9 – Sequence of U-band interferometric gain solutions with noise diode alternately on and off.

4 POTENTIAL CONSEQUENCES FOR USERS

Observed nonlinear effects described in Section 2 may in principle influence telescope users as described below. The listed items represent potential consequences that, unless noted otherwise, have not yet been verified or characterised in detail:

- False positive candidates may be detected by pulsar search algorithms as a result of periodic power variation in RFI, in particular detections at cellular RFI frame and code periods, or multiples thereof. This effect has been reported by users.
- Increased calibration error and reduction in imaging dynamic range may occur, as well as increased error in absolute flux calibration and measurement. This may occur if significant differences in T_{SYS} are present between science fields and calibrator fields. Strong satellite RFI may lead to significant error on individual scans.
- Variation in T_{SYS}, use of the noise diode, and satellite RFI are expected to be sources of gain error in Intensity Mapping observations.
- Measurement of noise diode power variation is expected to be less accurate, as demonstrated in Section 2.2, reducing its usefulness as a means to track changes in receiver gain.
- Polarisation characteristics of beamformer beams may vary due to changes in individual receiver gains in response to bright satellite RFI. Applying polarisation calibration solutions solved on one pulsar to another may result in slight inaccuracy if there are significant differences in T_{SYS} between target pointings. Problems previously experienced with noise diode over-polarisation within pulsar polarisation calibration may be ascribed to gain variation due to noise diode firing. Small errors in pulsar flux calibration would be expected with significant T_{SYS} differences between the calibrator and science field.
- Increased error in selected telescope performance and calibration measurements is expected, e.g.:
    - 'Y-factor' measurements that utilise large differences in T_{SYS} and / or the noise diode, e.g. antenna SEFD measurements, are expected to contain errors of a few percent.
    - Gain variation due to T_{SYS} and satellite RFI is expected to be a source of error in interferometric pointing calibration measurements.
    - A GNSS satellite crossing antenna main beams during phase-up calibration may result in individual antennas contributing unequal power to the beamformer summation.

5 POSSIBLE MITIGATION

The following methods to mitigate the observed nonlinearity are currently being considered.

5.1 INCREASE IN NOMINAL POWER LEVELS

As noted in the Digitiser investigation [5], ADCs tend to have lower harmonics at higher input power, and hence should have improved linearity at higher nominal input power levels. At present,

both L-band and U-band nominal ADC input power is set fairly low to leave significant headroom for RFI. Due to limited gain on the L-band digitiser, increasing the nominal input power is unfortunately only possible for the U-band Digitiser.

The median ratio across all antennas between $|g_{ON}|^2$ and $|g_{OFF}|^2$, respectively interferometric gain when the noise diode is on and off, was measured for U-band at different nominal ADC input powers by adjusting RFCU attenuation. Results are shown in Figure 10.

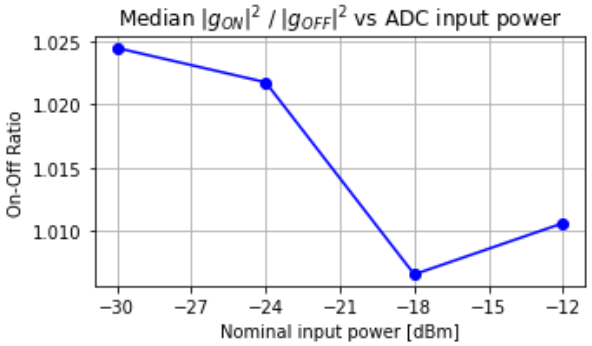

Figure 10 – Ratio of gains with noise diode on vs. off at different nominal ADC input power levels.

Results are promising and suggest that the magnitude of nonlinear effects may be reduced by 50% or more by increasing input power levels to the ADC. Increasing power levels may however lead to greater frequency of ADC saturation events due to RFI. A sensible trade-off hence needs to be set between increasing power levels while keeping number of saturation events at an acceptable level.

5.2 FLAGGING

Offsets of satellite positions from antenna pointing directions are easily calculated from published TLE databases. Correlator data may hence be flagged, either during or after observations, at times when selected satellites are within a specified offset from the pointing direction. This would indicate that gain instability is present and data should be considered suspect.

GNSS constellation satellites are the primary concern, though selected other constellations, e.g. NOAA and GOES, also transmit strong RFI. Some GNSS constellations, e.g. Beidou and Galileo, are sufficiently bright to cause gain variation in antenna sidelobes. A database would hence need to be set up of strong satellite RFI emitters and the offset from pointing direction within which each should be flagged.

5.3 GAIN CORRECTION

The curves of gain variation vs ADC output power provided in Figure 2 suggest that correction of gain variation at correlator output may be possible in principle. ADC output power is already stored as a sensor, however careful consideration would need to be given to calculation of stable, accurate correction curves.

Correction at correlator output would not address gain variation in beamformer data, and the best location to correct for nonlinearity would be at ADC output. The investigation in [5] suggests that

ADC nonlinearity is modelled to reasonable accuracy with memoryless nonlinear mapping. This leaves open the possibility of simple corrective mapping and / or harmonic cancellation schemes. Characterising the ADC nonlinearity to sufficient accuracy was however found to be challenging, and further investigation is required.

6 FUTURE WORK

Future work will focus on resolving remaining questions about the nonlinear mechanism noted in Section 3, as well as investigating and implementing possible compensation mechanisms. Detailed characterisation of potential consequences for users may be investigated in selected cases.

REFERENCES

[1] S. Salie, "*MeerKAT Telescope Compression Level Tests*", M0000-0000-076, NRF, Rev 1.

[2] A. Peens-Hough, P. Herselman, T. Küsel, "*MeerKAT System Description: Receptor Description and Requirements*", M0000-0000V1-37 TM, NRF, Rev 5.

[3] M Gouws, "*System-level Characterisation of MeerKAT L-band Receiver Nonlinearity*", M0000-00000-077, NRF, Rev 1.

[4] M Gouws, "*System-level Characterisation of MeerKAT UHF-band Receiver Nonlinearity*", M000-0000-079, NRF, Rev 1.

[5] M Gouws and R. Ebrahim, "*Characterisation of MeerKAT Digitiser Nonlinearity*", M1130-0000-037, NRF, Rev 1.

Overview of MeerKAT L-band and U-band Nonlinearity Rev 1

Final Audit Report 2021-02-05

Created:	2021-02-05
By:	Sulayman Salie (ssalie@ska.ac.za)
Status:	Signed
Transaction ID:	CBJCHBCAABAAYmxq7J4fDzlKTyTSmU5CbH2WlQ2Z8ig-

"Overview of MeerKAT L-band and U-band Nonlinearity Rev 1" History

Document created by Sulayman Salie (ssalie@ska.ac.za)
2021-02-05 - 2:59:08 PM GMT- IP address: 129.205.181.230

Document emailed to Marcel Gouws (mgouws@ska.ac.za) for signature
2021-02-05 - 2:59:46 PM GMT

Email viewed by Marcel Gouws (mgouws@ska.ac.za)
2021-02-05 - 7:53:19 PM GMT- IP address: 66.249.93.202

Document e-signed by Marcel Gouws (mgouws@ska.ac.za)
Signature Date: 2021-02-05 - 7:53:52 PM GMT - Time Source: server- IP address: 196.24.39.242

Agreement completed.
2021-02-05 - 7:53:52 PM GMT